AIMS Mathematics

http://www.aimspress.com/journal/Math

AIMS Mathematics, 5(5): 5287–5308.
DOI:10.3934/math.2020339
Received: 28 March 2020
Accepted: 10 June 2020
Published: 19 June 2020

Research article

Numerical solution of the linear time fractional Klein-Gordon equation using transform based localized RBF method and quadrature

Xiangmei Li[1], Kamran[2], Absar Ul Haq[3] and Xiujun Zhang[4,*]

[1] School of Cybersecurity, Chengdu University of Information Technology, Chengdu, 610225, China
[2] Department of Mathematics, Islamia College Peshawar, Khyber Pakhtoon Khwa, Pakistan
[3] Department of Basic Science and Humanities, University of Engineering and Technology, Lahore (Narowal Campus), Pakistan
[4] Key Laboratory of Pattern Recognition and Intelligent Information Processing, Institutions of Higher Education of Sichuan Province, Chengdu University, Chengdu, 610106, China

* **Correspondence:** Email: woodszhang@cdu.edu.cn.

Abstract: This work aims to approximate the solution of the linear time-fractional Klein-Gordon equations in Caputo's sense. The Laplace transform is applied to linear time fractional Klein-Gordon equation to eliminate the time variable and avoid the time stepping procedure. Application of the Laplace transform avoids the time instability issues which commonly occurs in time stepping methods and reduces the computational cost. The transform problem is then solved using local RBFs and finally the solution is obtained by the inverse Laplace transform. The solution is represented as an integral along a smooth curve in the complex plane which is then approximated by quadrature rule. The proposed method is capable of solving linear time fractional partial differential equations. The stability and convergence of the method are discussed. The efficiency of the method is demonstrated with the help of numerical experiments.

Keywords: Klein-Gordon equations; Caputo's time fractional derivative; Laplace transform; local RBF method; contour integration; quadrature rule
Mathematics Subject Classification: 26A33, 65M12, 65R10, 81Q05

1. Introduction

Fractional calculus have recently become a fascinating field of study due to its vast applications in various aspects of modern life. It has been observed that many physical phenomena can be modeled successfully by means of fractional order differential equations, where the integer-order differential equations fails in modeling certain issues [1]. Compared to integer order derivatives some properties

of the non-integer order derivatives are very tedious to deal with. Thus, it becomes of great importance to establish more results for fractional calculus. Recently lots of researchers have proposed new and efficient analytical and numerical schemes to approximate the solutions of numerous fractional order problems. In this connection one can find efficient work done by researchers such as the analysis of fractional Drinfeld-Sokolov-Wilson model with exponential memory [2], a homotopy perturbation sumudu transform method (HPSTM) for solving fractional equal width (EW) equation [3]. The ternary-fractional differential transform method, that extends its applicability to encompass initial value problems in the fractal 3D space [1]. The local fractional homotopy perturbation Sumudu transform scheme and the local fractional reduced differential transform method for a fractal vehicular traffic flow problem [4]. The authors in [5] have proposed a numerical algorithm based on homotopic technique to examine the fractional vibration equation in Atangana-Baleanu sense. The authors in [6] have presented the efficiency of the Atangana-Baleanu (AB) derivative over Caputo-Fabrizio (CF) to some nonlinear partial differential equations. The authors in [7] have done a comparative analysis of exothermic reactions model having constant heat source in the porous media via Caputo, Caputo Fabrizio and Atangana-Baleanu theories. In [8] a hybrid numerical scheme based on the homotopy analysis transform method (HATM) to examine the fractional model of nonlinear wave-like equations having variable coefficients is presented. The Klein-Gordon is one of the most important mathematical model which finds its applications in numerous phenomenon in science and engineering. It has been applied to non linear optics, quantum field theory, Plasma physics, fluid dynamics, chemical kinetics and solid state physics [9–11]. In literature a lot of work has been done on solving the Klein-Gordon equation analytically some of them are the tanh and the sine-cosine methods [12], the differential transform method [13], Modified Kudryashov method [14, 15], ansatz method [16], $\mathrm{Exp}(-\phi(\epsilon))$-expansion method [17], and the variational iteration method [18]. The residual power series method for linear time fractional Klein-Gordon equation [19], homotopy analysis method [20, 21], local fractional series expansion method [10], homotopy perturbation method [22], and the fractional Riccati expansion method [23]. In [24] a hybrid method based on local fractional Sumudu transform method and homotopy perturbation technique is employed to find the non differentiable solution of Klein-Gordon equation on Cantor sets. Since Most of the problems cannot be solved analytically so one must use numerical methods. Despite the fact that, numerical approximation of these equations are rare, in literature some excellent work is available, such as Mohebi et al utilized the Compact finite difference method [25] and the implicit RBF meshless method [26] for the approximation of linear time fractional Klein-Gordon equations. M. M. Khader [27] applied an efficient method based on the generalized laguerre polynomials for approximating the linear time fractional Klein-Gordon equations. In [28] the authors used the wavelet method for approximating a class of fractional Klein-Gordon equations. The authors in [29] proposed a numerical algorithm based on the applications of the operational matrices of the Legendre scaling functions for the approximation of fractional Klein-Gordon equation. The authors in [30] applied a high order compact finite difference scheme to two dimensional fractional Klein-Gordon equations. Dehghan et al [31] used radial basis functions to approximate the solution of non linear Klein-Gordon equations. However in these time stepping schemes the computations may be very expansive because each new iteration is dependent on the previous time step. An alternative way is to use the Laplace transform coupled with these numerical methods. In literature one can find numerous research work on the coupling of other numerical methods and Laplace transform. The

Laplace transform was first coupled with the boundary integral method by Rizzo and Shippey [32]. Moridis and Reddell coupled Laplace transform with finite difference, boundary element and finite element methods [33–35]. In [36] the authors coupled the Galerkin method with Laplace transform. Moridis and Kansa [37] coupled multiquadric method and Laplace transform for the approximation of PDEs. In [38] the author studied RBF method coupled with Laplace transform on unit sphere. Similarly the coupling of Laplace transform with other numerical methods such as spectral method, finite difference method, boundary particle method, RBF method, and the finite element method can be found in [39–44] and the references therein. In this work we apply the idea of [45, 46], the Laplace transform is coupled with local RBF method to approximate linear time-fractional Klein-Gordon equation. The Laplace transform is used to avoid the stability restrictions, which are commonly encountered in time-stepping procedure. The local radial basis function method is used to resolve the issue of ill-conditioning of the differentiation matrices and the sensitivity of shape parameter in global radial basis functions method. The main idea of the local radial basis function method is the collocation on overlapping sub-domains of the whole domain. The overlapping sub-domains remarkably reduce the size of collocation matrix by solving many small size matrices. Each small matrix has the same size as the number of nodes in the domain of influence of each node. In order to validate our method we consider linear time-fractional Klein-Gordon equation of the form [25]

$$\begin{aligned}&\beta^{\alpha-1}\frac{\partial^\alpha \chi(\mathbf{x},t)}{\partial t^\alpha}+\eta\frac{\partial \chi(\mathbf{x},t)}{\partial t}+\kappa\chi(\mathbf{x},t)\\&=\mathcal{L}\chi(\mathbf{x},t)+\beta^{\alpha-1}f(\mathbf{x},t),\\&0\le \mathbf{x}\le L,\ 1<\alpha\le 2,\ 0\le t\le 1, \eta\ge 0, \kappa\ge 0,\end{aligned}\tag{1.1}$$

with initial and boundary conditions given in (1.2) and (1.3),

$$\chi(\mathbf{x},0)=f_1(\mathbf{x}),\ \frac{\partial \chi(\mathbf{x},t)}{\partial t}|_{t=0}=f_2(\mathbf{x}),\ \mathbf{x}\in\Omega,\tag{1.2}$$

$$\mathcal{B}\chi(\mathbf{x},t)=h(t),\ \mathbf{x}\in\partial\Omega.\tag{1.3}$$

Here $\mathcal{L}$ and $\mathcal{B}$ are the governing and boundary differential operators, and $\frac{\partial^\alpha}{\partial t^\alpha}$ is the Caputo fractional derivative of order α defined by [47]:

$$\begin{aligned}&\frac{\partial^\alpha}{\partial t^\alpha}\chi(t)\\&=\frac{1}{\Gamma(p-\alpha)}\int_0^t (t-s)^{m-\alpha-1}\frac{d^m}{ds^m}\chi(s)ds,\\&m-1\le\alpha\le m,\ m\in\mathbf{N}.\end{aligned}\tag{1.4}$$

Let the Laplace transform of $\chi(t)$ be denoted and defined by

$$\hat{\chi}(s)=L\{\chi(t)\}=\int_0^\infty e^{-st}\chi(t)dt,\tag{1.5}$$

and the Laplace transform of the Caputo derivative is defined by

$$L\{\frac{\partial^\alpha}{\partial t^\alpha}\chi(t)\}=s^\alpha\hat{\chi}(s)-\sum_{i=0}^{m-1}s^{\alpha-i-1}\chi^{(i)}(0).\tag{1.6}$$

2. Proposed scheme

Here we construct a local RBF method coupled with Laplace transform for the approximation of the solution of the linear time-fractional Klein-Gordon equations. In order to avoid the time stepping procedure the Laplace transform is used to eliminate the time variable. Then the local RBF method is utilized to approximate the time independent linear PDE.

Applying the Laplace transform to Eqs (1.1) and (1.3), we get

$$\begin{aligned}&\beta^{\alpha-1}\left(s^{\alpha}\hat{\chi}(\mathbf{x},s)-s^{\alpha-1}\chi(\mathbf{x},0)-s^{\alpha-2}\chi_t(\mathbf{x},0)\right)\\&+\eta\left(s\hat{\chi}(\mathbf{x},s)-\chi(\mathbf{x},0)\right)+\kappa\hat{\chi}(\mathbf{x},s)\\&=\mathcal{L}\hat{\chi}(\mathbf{x},s)+\beta^{\alpha-1}\hat{f}(\mathbf{x},s),\end{aligned}\tag{2.1}$$

thus we have the following linear system

$$\left(\beta^{\alpha-1}s^{\alpha}I+\eta sI+\kappa I-\mathcal{L}\right)\hat{\chi}(\mathbf{x},s)=\hat{g}(\mathbf{x},s),\ \mathbf{x}\in\Omega,\tag{2.2}$$

$$\mathcal{B}\hat{\chi}(\mathbf{x},s)=h(s),\ \mathbf{x}\in\partial\Omega,\tag{2.3}$$

where

$$\begin{aligned}&\hat{g}(\mathbf{x},s)=\beta^{\alpha-1}s^{\alpha-1}\chi(\mathbf{x},0)\\&+\beta^{\alpha-1}s^{\alpha-2}\chi_t(\mathbf{x},0)+\eta\chi(\mathbf{x},0)+\beta^{\alpha-1}\hat{f}\chi(\mathbf{x},s).\end{aligned}$$

In the following section the local RBF method is used to approximate the differential operator $\mathcal{L}$ and $\mathcal{B}$ in order to solve the problem (2.2)–(2.3) in Laplace space.

2.1. Local RBF method

In local RBF method the approximation of the function $\hat{\chi}(\mathbf{x})$, for a given set of data points $\{\hat{\chi}(\mathbf{x}_i) : i = 1, ..., N\}$, where $\{\mathbf{x}_i : i = 1, ..., N\} \subset \Omega \subset \mathcal{R}^d,\ d \geq 1$ takes the form

$$\hat{\chi}(\mathbf{x}_i)=\sum_{\mathbf{x}_j\in\Omega_i}\lambda_j\phi(\|\mathbf{x}_i-\mathbf{x}_j\|),\tag{2.4}$$

where $\boldsymbol{\lambda}^i = \{\lambda^i_j : j = 1, ..., n\}$ is the vector of expansion coefficients, $\phi(r),\ r \geq 0$ is radial kernel and the distance between the centers $\mathbf{x}_i$ and $\mathbf{x}_j$ is $r = \|\mathbf{x}_i - \mathbf{x}_j\|$, and Ω_i is a sub domain of Ω containing $\mathbf{x}_i$, and around $\mathbf{x}_i$ it contains n neighboring centers. So we have N number of $n \times n$ linear systems given by

$$\hat{\chi}^i=\Phi^i\boldsymbol{\lambda}^i, i=1,2,3,...,N,\tag{2.5}$$

the elements of the interpolation matrix Φ^i are $b^i_{kj} = \phi(\|\mathbf{x}_k - \mathbf{x}_j\|)$, where $\mathbf{x}_k, \mathbf{x}_j \in \Omega_i$, each $n \times n$ system is then solved for the unknowns $\boldsymbol{\lambda}^i = \{\lambda^i_j : j = 1, ..., n\}$. Next the operator $\mathcal{L}\hat{\chi}(\mathbf{x})$, is approximated by

$$\mathcal{L}\hat{\chi}(\mathbf{x}_i)=\sum_{\mathbf{x}_j\in\Omega_i}\boldsymbol{\lambda}^i_j\mathcal{L}\phi(\|\mathbf{x}_i-\mathbf{x}_j\|),\tag{2.6}$$

the above Eq (2.6) can be expressed as

$$\mathcal{L}\hat{\chi}(\mathbf{x}_i)=\boldsymbol{\lambda}^i\cdot\boldsymbol{\nu}^i,\tag{2.7}$$

where $\boldsymbol{\nu}^i$ is of order $1 \times n$ and $\boldsymbol{\lambda}^i$ of order $n \times 1$, the entries of $\boldsymbol{\nu}^i$ are shown in the following equation

$$\boldsymbol{\nu}^i = \mathcal{L}\phi(\|\mathbf{x}_i - \mathbf{x}_j\|),\ \mathbf{x}_j \in \Omega_i, \tag{2.8}$$

using Eq (2.5), the coefficients $\boldsymbol{\lambda}^i$ can be eliminated as,

$$\boldsymbol{\lambda}^i = (\Phi^i)^{-1}\hat{\boldsymbol{\chi}}^i, \tag{2.9}$$

using the values of $\boldsymbol{\lambda}^i$ from (2.9) in (2.7) we get,

$$\mathcal{L}\hat{\chi}(\mathbf{x}_i) = \boldsymbol{\nu}^i(\Phi^i)^{-1}\hat{\boldsymbol{\chi}}^i = \mathbf{w}^i\hat{\boldsymbol{\chi}}^i \tag{2.10}$$

where,

$$\mathbf{w}^i = \boldsymbol{\nu}^i(\Phi^i)^{-1}, \tag{2.11}$$

Hence the linear differential $\mathcal{L}$ is approximated using the local RBF method for each center $\mathbf{x}_i$ as

$$\mathcal{L}\hat{\chi} \equiv \mathbf{D}\hat{\chi}. \tag{2.12}$$

The matrix $\mathbf{D}$ is sparse differentiation matrix which approximates the linear differential operator $\mathcal{L}$. The matrix $\mathbf{D}$ has order $N \times N$ which contains n non-zero and $N - n$ zero entries, where n is the number of centers in the sub domain Ω_i. The same procedure can be applied to the boundary operator $\mathcal{B}$.

2.2. Selecting good value of shape parameter

In literature a large number of radial kernels are available. In this article we have selected the multi-quadrics $\phi(r) = \sqrt{1 + (rc)^2}$ for our numerical approximation. The accuracy of the numerical solution greatly depends on the parameter c. The researchers always search for that value of c which gives an optimal solution. In this regard a large amount of work has been done such as [48–50] and references therein . Here we utilize the uncertainty principle [51] for optimal shape parameter c.

Algorithm:

- The interval $10^{12} < Cond < 10^{16}$ is selected for the condition number (Cond) of the system matrices of the given problem.
- Using SVD, the interpolation matrix is decomposed as $\mathbf{R}, \mathbf{P}, \mathbf{Q} = svd(\Phi^i)$. The order of Φ^i is $n \times n$ (n is the number of centers in each Ω_i), and the n singular values of the matrix Φ^i lies on the diagonal of the matrix $\mathbf{P}$ ($\mathbf{P}$ is a diagonal matrix), and the condition number of Φ^i is $Cond = \|\Phi^i\|\|(\Phi^i)^{-1}\| = \frac{\max(\mathbf{P})}{\min(\mathbf{P})}$.

- The c is searched until the condition $10^{12} < Cond < 10^{16}$ is satisfied, the algorithm is given as
  Step 1: set $Cond = 1$
  Step 2: select $10^{12} < Cond < 10^{16}$
  Step 3: while $Cond > Cond_{max}$ and $Cond < Cond_{min}$
  Step 4: $\mathbf{R}, \mathbf{P}, \mathbf{Q} = svd(\Phi^i)$
  Step 5: $Cond = \frac{\max(\mathbf{P})}{\min(\mathbf{P})}$
  Step 6: if $Cond < Cond_{min},\ c = c - \delta c$
  Step 7: if $Cond > Cond_{max},\ c = c + \delta c$

c (optimal) = c.

Optimal value of the parameter c is obtained, when the above condition is satisfied, and then we can compute the inverse using $(\Phi^i)^{-1} = (\mathbf{RPQ^T})^{-1} = \mathbf{QP}^{-1}\mathbf{R}^T$ [52]. Hence $\mathbf{w}^i$ in (2.11) can be computed.

Following the discretization by local RBF method of the linear differential and boundary operators $\mathcal{L}$ and $\mathcal{B}$ respectively, the system (2.2)–(2.3) is solved for each point s. Finally the solution of the problem (1.1)–(1.3) is obtained using the inverse of Laplace transform

$$\chi(\mathbf{x}, t) = \frac{1}{2\pi i}\int_{\sigma-i\infty}^{\sigma+i\infty} e^{st}\hat{\chi}(\mathbf{x}, s)ds. \tag{2.13}$$

In applying the Laplace transform method the calculation of inverse Laplace transform is the main difficulty. In many cases it is difficult to find the inverse Laplace transform analytically so numerical methods must be used. A large number of methods for the numerical inversion of Laplace transform have been developed. In this work we use the idea of [39, 42] in which the integration is performed over a parabolic or hyperbolic path Γ, so the integral in equation (2.13) can be written as

$$\chi(\mathbf{x}, t) = \frac{1}{2\pi i}\int_{\Gamma} e^{st}\hat{\chi}(\mathbf{x}, s)ds, \quad \sigma > \sigma_0, \tag{2.14}$$

where Γ is a path of integration joining $\sigma - i\infty$ to $\sigma + i\infty$ and

$$s = s(\omega), \tag{2.15}$$

using (2.15) in (2.14), we find the following expression

$$\chi(\mathbf{x}, t) = \frac{1}{2\pi i}\int_{-\infty}^{\infty} e^{s(\omega)t}\hat{\chi}(\mathbf{x}, s(\omega))\acute{s}(\omega)d\omega, \tag{2.16}$$

Finally the trapezoidal rule with uniform step size k is used to approximate (2.16), as

$$\chi_k(\mathbf{x}, t) = \frac{k}{2\pi i}\sum_{j=-M}^{M} e^{s_j t}\hat{\chi}(\mathbf{x}, s_j)\acute{s}_j, \quad s_j = s(\omega_j), \omega_j = jk. \tag{2.17}$$

3. Error analysis

The approximate solution of the proposed scheme is defined by Eq (2.17). The accuracy of (2.17) greatly depends on the path of the integration Γ. There are various contours available in the literature. Recently the hyperbolic [41] and parabolic [42] contours are used to approximate the integer and fractional order PDEs. In our computations the hyperbolic path due to [41] is used.

$$s(\omega) = \eta + \gamma\,(1 - sin(\delta - \iota\omega))\,, \text{ for } \omega \in \mathcal{R}, \quad (\Gamma) \tag{3.1}$$

where $\eta \geq 0$, $\gamma > 0$, $\frac{1}{2}\pi < \beta < \pi$, and $0 < \delta < \beta - \frac{1}{2}\pi$. In fact, when we choose $Im\ \omega = \lambda$, the Eq (3.1) is reduced to the left branch of the hyperbola

$$\left(\frac{x - \gamma - \eta}{\gamma\sin(\delta + \lambda)}\right)^2 - \left(\frac{y}{\gamma\cos(\delta + \lambda)}\right)^2 = 1, \tag{3.2}$$

transforming the strip $Z_r = \{\omega : Im\ \omega \leq r, r > 0\}$ into the hyperbola $\Omega_r = \{s : \omega \in Z_r\} \supset \Gamma$. Suppose $\Sigma_\phi = \{s \neq 0 : |args| \leq \phi\} \cup 0,\ 0 < \phi < \frac{(1-\alpha)\phi}{2}$, and let $\Sigma_\beta^\eta = \eta + \Sigma_\beta, \Gamma \subset \Omega_r \subset \Sigma_\beta^\eta$. The following theorem gives the error estimate of the scheme for the contour Γ.

Theorem 3.1 ([41], Theorem 2.1) let the solution of (1.1) be $\chi(\mathbf{x}, t)$, with $\hat{f}(\mathbf{x}, t)$ analyitc in Σ_β^η. Let $\Gamma \subset \Omega_r \subset \Sigma_\beta^\eta$, and $b > 0$ be defined by $b = cosh^{-1}(\frac{1}{\theta\tau \sin(\delta)})$, where $\tau = \frac{t_0}{T}$, $0 < \theta < 1$, $0 < t_0 < T$, and let $\gamma = \frac{\theta\bar{r}M}{bT}$. Then for the approximate solution defined by (2.17), with $k = \frac{b}{M} \leq \frac{\bar{r}}{log2}$, $|\chi(\mathbf{x}, t) - \chi_k(\mathbf{x}, t)| \leq \left(\|\chi_0\| + \|\hat{f}(\mathbf{x}, t)\|_{\Sigma_\beta^\eta}\right) CQe^{\eta\tau} g(\rho_r M)e^{-\mu M}$, for $\mu = \frac{\bar{r}(1-\theta)}{b}$, $\rho_r = \frac{\theta\bar{r}\tau \sin(\delta - r)}{b}$, $g(x) = \max(1, log(\frac{1}{x}))$, $\bar{r} = 2\pi r$, $r > 0$,$C = C_{\delta,r,\beta}$, and $t_0 \leq t \leq T$. Thus the corresponding error estimate is of the order

$$\text{Error Estimate} = |\chi(\mathbf{x}, t) - \chi_k(\mathbf{x}, t)| = O(g(\rho_r M)e^{-\mu M}).$$

4. Stability analysis

In order to investigate the systems (2.2)–(2.3) stability, we represent the system in discrete form as

$$Y\hat{\chi} = \mathbf{b}, \tag{4.1}$$

where Y is the sparse differentiation matrix of order $N \times N$ obtained using local RBF method. For the system (4.1) the constant of stability is given by

$$C = \sup_{\hat{\chi} \neq 0} \frac{\|\hat{\chi}\|}{\|Y\hat{\chi}\|}, \tag{4.2}$$

where C is finite using any discrete norm $\|.\|$ on R^N. From (4.2) we may write

$$\|Y\|^{-1} \leq \frac{\|\hat{\chi}\|}{\|Y\hat{\chi}\|} \leq C, \tag{4.3}$$

Similarly for the pseudoinverse $Y^\dagger$ of Y, we can write

$$\|Y^\dagger\| = \sup_{v \neq 0} \frac{\|Y^\dagger v\|}{\|v\|}. \tag{4.4}$$

Thus we have

$$\|Y^\dagger\| \geq \sup_{v = Y\hat{\chi} \neq 0} \frac{\|Y^\dagger Y\hat{\chi}\|}{\|Y\hat{\chi}\|} = \sup_{\hat{\chi} \neq 0} \frac{\|\hat{\chi}\|}{\|Y\hat{\chi}\|} = C. \tag{4.5}$$

We can see that Eqs (4.3) and (4.5) confirms the bounds for the stability constant C. Calculating the pseudoinverse for approximating the system (4.1) numerically may be very expansive computationally, but it ensures the stability. The MATLAB's function condest can be used to estimate $\|Y^{-1}\|_\infty$ in case of square systems, thus we have

$$C = \frac{condest(Y')}{\|Y\|_\infty} \tag{4.6}$$

This work well with less number of computations for our sparse differentiation matrix Y. Figures 1 and 2 show the bounds for the constant C of our system (2.2)–(2.3) for Problem 3. Selecting $N = 50$,

$M = 80$,$n = 15$, and $\alpha = 0.8$ at $t = 1$, we have $1 \leq C \leq 1.1620$. It is observed that the stability constant is bounded by very small numbers, which guarantees the stability of the proposed local RBF scheme.

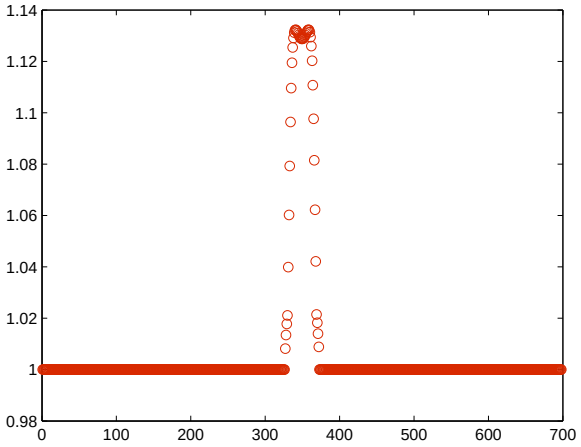

Figure 1. The stability constant C is shown for our differentiation matrix Y corresponding to problem 3, obtained using $N = 70, n = 10, M = 50$, and $\alpha = 0.85$.

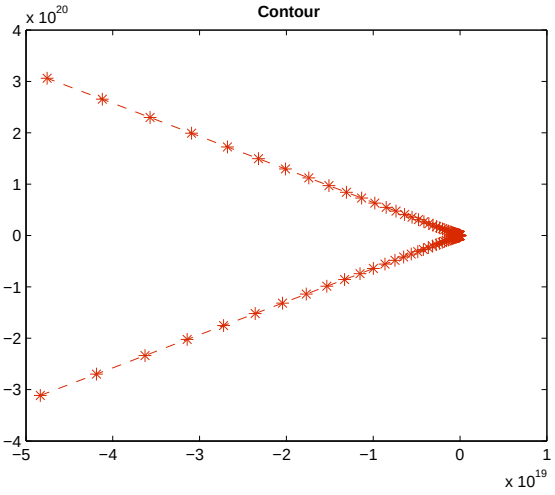

Figure 2. The contour of integration is shown for the Problem 3 for $M = 50$.

5. Numerical results

This section is devoted to the numerical experiments. The proposed method is tested here for 1-D time fractional order Klein-Gordon equations. The multi-quadrics radial kernels $\phi(r) = (1 + (rc)^2)^{1/2}$ are used in all our numerical experiments. The Uncertainty principle [51] is used to optimize the shape parameter c . The accuracy of the method is measured using L_∞ error defined by

$$L_\infty = \|\chi(\mathbf{x}, t) - \chi_k(\mathbf{x}, t)\|_\infty = \max_{1 \leq j \leq N} (|\chi(\mathbf{x}, t) - \chi_k(\mathbf{x}, t)|)$$

is used. Here χ_k and χ are the numerical and exact solutions respectively.

5.1. Problem 1

If we use $\beta = 1$, $\kappa = 1$, and $\eta = 0$, Eq (1.1) takes the form

$$\frac{\partial^\alpha \chi(x,t)}{\partial t^\alpha} + \chi(x,t) - \frac{\partial^2 \chi(x,t)}{\partial x^2} = f(x,t), \tag{5.1}$$

where $1 \leq \alpha \leq 2,\ t \geq 0,\ 0 \leq x \leq 1$, with zero boundary and initial conditions. The domain $[0,1]$ is selected for the problem with exact solution

$$\chi(x,t) = t^2(e - e^x)\sin(x),$$

and non homogeneous term

$$\begin{aligned} f(x,t) &= \frac{2t^{2-\alpha}}{(2-\alpha)\Gamma(2-\alpha)}(e - e^x)\sin(x) + t^2(2e - e^x)\sin(x) \\ &\quad +2t^2 e^x \cos(x). \end{aligned}$$

The MATLAB's command $\omega = -M : k : M$ is used to generate the quadrature points along the path of integration Γ. The parameters used in our computations are $\alpha = 1.75, \eta = 2, \tau = \frac{t0}{T}, r = 0.1387, \theta = 0.1, \delta = 0.1541, t_0 = 0.5$ and $T = 5$. Using Eq (3.1) the remaining optimal parameters can be found for the hyperbolic path Γ. In our computations $n = 6$ in the sub domain Ω_i and $N = 40$ in the global domain Ω are selected. The error estimates and L_∞ errors are shown in Tables 1 and 2. The efficiency of the method can be seen in the results. The actual error and error estimates are shown in Figure 3 and the absolute errors for different values of α are shown in Figure 4. The numerical and the exact solutions are shown in Figures 5 and 6 respectively.

Table 1. Approximate solution for Problem 1 at $t = 1$, and $1\times 10^{12} \leq \kappa \leq 1\times 10^{16}$, in the domain $[0,1]$.

$N = 60$, $n = 5$ $\alpha = 1.25$	M	L_∞ Error (Γ)	Error Estimate (Γ)	CPU time(s)
	10	7.65×10^{-4}	4.4187	0.145896
	15	2.30×10^{-3}	2.6363	0.158580
	20	1.30×10^{-3}	1.5582	0.169243
	30	1.38×10^{-4}	0.5373	0.218606
	40	6.57×10^{-6}	0.1836	0.384568
	50	1.25×10^{-5}	0.0625	0.682311
	60	9.58×10^{-6}	0.0212	1.143210
	70	9.70×10^{-6}	0.0072	2.792846
	80	9.66×10^{-6}	0.0024	5.805704
[25] 1.34×10^{-6}				

Table 2. Approximate solution for Problem 1 at $t = 1$, and $1\times 10^{12} \leq \kappa \leq 1\times 10^{16}$, in the domain [0, 1].

$N = 60$, $n = 5$ $\alpha = 1.75$	M	L_∞ Error (Γ)	Error Estimate (Γ)	CPU time(s)
	10	7.65×10^{-4}	4.4187	0.151320
	15	2.30×10^{-3}	2.6363	0.190760
	20	1.30×10^{-3}	1.5582	0.173974
	30	1.38×10^{-4}	0.5373	0.275586
	40	6.35×10^{-6}	0.1836	0.483761
	50	1.19×10^{-5}	0.0625	0.732991
	60	8.99×10^{-6}	0.0212	1.269992
	70	9.11×10^{-6}	0.0072	3.328360
	80	9.07×10^{-6}	0.0024	5.789626
[25] 4.45×10^{-5}				

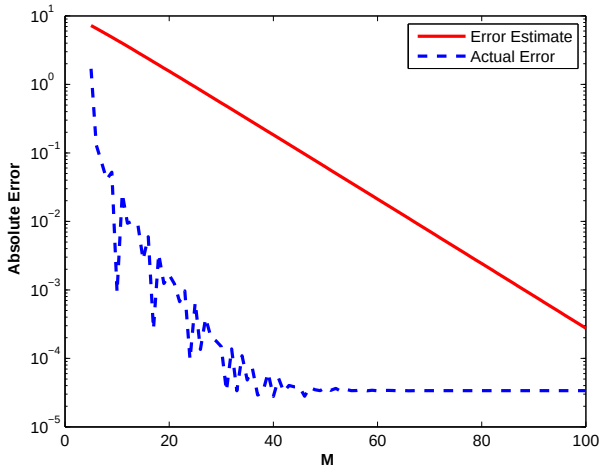

Figure 3. Plot of Actual error and Error Estimate corresponding to problem 1 obtained using $N = 90$ nodes in the global domain, $n = 10$ nodes in the local domain, fractional order $\alpha = 1.85$, at $t = 1$. The figure illustrate that the convergence rate of the numerical computation of inverse Laplace transform is inline with the Error Estimate (theoretical bound).

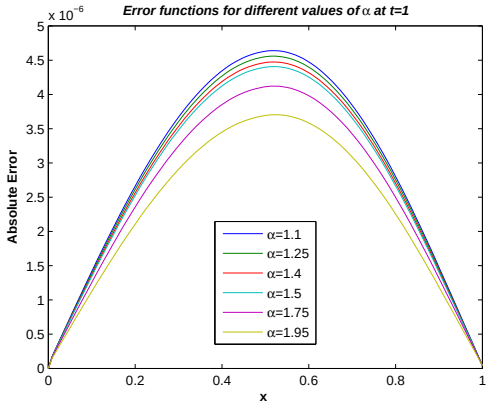

Figure 4. The absolute errors for different values of α are shown. It is observed that the error decreases with increasing the value of fractional order α.

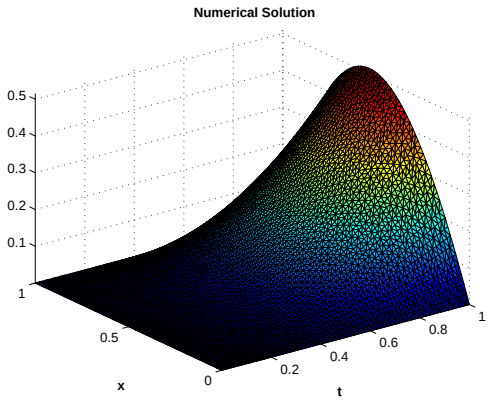

Figure 5. The numerical solution obtained using $N = 70$ nodes in global domain, $n = 10$ nodes in local domain, $M = 30$, and fractional order $\alpha = 1.95$.

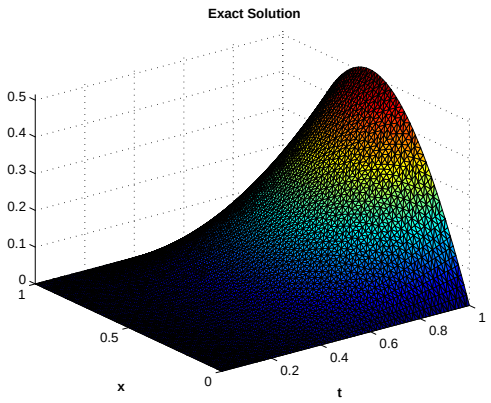

Figure 6. The exact solution obtained using $N = 70$ nodes in global domain, $n = 10$ nodes in local domain,$M = 30$, and fractional order $\alpha = 1.95$.

5.2. Problem 2

If we use $\beta = 1$, $\kappa = 1$, and $\eta = 1$, Eq (1.1) takes the form

$$\frac{\partial^\alpha \chi(x,t)}{\partial t^\alpha} + \frac{\partial \chi(x,t)}{\partial t} + \chi(x,t) = \frac{\partial^2 \chi(x,t)}{\partial x^2} + f(x,t), \tag{5.2}$$

where $1 \leq \alpha \leq 2,\ t \geq 0,\ 0 \leq x \leq 1$, with zero initial and boundary conditions, the exact solution of the problem is

$$\chi(x,t) = t^2 x \sin(x-1),$$

and non homogeneous term is

$$\begin{aligned} f(x,t) &= \frac{2t^{2-\alpha}}{(2-\alpha)\Gamma(2-\alpha)} x\sin(x-1) + 2tx\sin(x-1) \\ &+t^2 x\sin(x-1) - t^2(2\cos(x-1) - x\sin(x-1)). \end{aligned}$$

The MATLAB's command $\omega = -M : k : M$ is used to generate the quadrature points along the path of integration Γ. The parameters used in our computations are $\alpha = 1.75, r = 0.1387, \delta = 0.1541, \theta = 0.1, \tau = \frac{t0}{T}, \eta = 2, t_0 = 0.5$ and $T = 5$. Using Eq (3.1) the remaining optimal parameters can be found for the hyperbolic path Γ. In our computations $n = 7$ centers in the sub domain Ω_i and $N = 50$ in the global domain Ω are selected. The error estimates and L_∞ errors are shown in Tables 3 and 4. Also the maximum absolute errors for different values of α are shown in Table 5, which shows the efficiency of the proposed method. The numerical and exact solutions of this problem are shown in Figures 7 and 8 respectively and plot of Actual error and Error Estimate corresponding to problem 2 are shown in Figure 9.

Table 3. Approximate solution for Problem 2 at $t = 1$, and $1\times 10^{12} \leq \kappa \leq 1\times 10^{16}$, in the domain $[0, 1]$.

$M = 80$, $n = 5$ $\alpha = 1.25$	N	L_∞ Error (Γ)	Error Estimate (Γ)	CPU time(s)
	10	5.77×10^{-5}	0.0024	0.561563
	20	1.27×10^{-5}	0.0024	1.125699
	30	3.55×10^{-6}	0.0024	1.252799
	40	2.43×10^{-6}	0.0024	2.716533
	50	2.87×10^{-6}	0.0024	4.686349
	60	3.78×10^{-6}	0.0024	6.319554
	80	8.38×10^{-6}	0.0024	8.773851
	90	8.20×10^{-7}	0.0024	9.862299
[25] 5.91×10^{-7}				

Table 4. Approximate solution for Problem 2 at $t = 1$, and $1\times 10^{12} \leq \kappa \leq 1\times 10^{16}$, in the domain $[0, 1]$.

$N = 50$, $n = 7$ $\alpha = 1.75$	M	L_∞ Error (Γ)	Error Estimate (Γ)	CPU time(s)
	10	3.32×10^{-4}	4.4187	0.146540
	15	9.63×10^{-4}	2.6363	0.160951
	20	5.71×10^{-4}	1.5582	0.170815
	30	6.70×10^{-5}	0.5373	0.212776
	40	7.76×10^{-6}	0.1836	0.361477
	50	4.25×10^{-6}	0.0625	0.585600
	60	5.48×10^{-6}	0.0212	1.047157
	70	5.42×10^{-6}	0.0072	1.872323
	80	5.44×10^{-6}	0.0024	4.417500
[25] 7.59×10^{-6}				

Table 5. The maximum absolute errors (L_∞ errors) for different values of α are shown for Problem 2. The computations are done at $t = 1$, and $1\times 10^{12} \leq \kappa \leq 1\times 10^{16}$, in the domain $[0, 1]$, selecting $N = 11, n = 5$, and $M = 60$.

x	$\alpha = 1.25$	$\alpha = 1.5$	$\alpha = 1.75$	$\alpha = 1.95$
0	1.463×10^{-6}	1.463×10^{-6}	1.463×10^{-6}	1.463×10^{-6}
0.1	1.353×10^{-6}	1.340×10^{-6}	1.326×10^{-6}	1.315×10^{-6}
0.2	1.155×10^{-6}	1.131×10^{-6}	1.104×10^{-6}	1.079×10^{-6}
0.3	9.710×10^{-7}	9.400×10^{-7}	9.010×10^{-7}	8.630×10^{-7}
0.4	8.170×10^{-7}	7.820×10^{-7}	7.360×10^{-7}	6.850×10^{-7}
0.5	6.760×10^{-7}	6.410×10^{-7}	5.910×10^{-7}	5.320×10^{-7}
0.6	5.180×10^{-7}	4.860×10^{-7}	4.370×10^{-7}	3.740×10^{-7}
0.7	3.510×10^{-7}	3.240×10^{-7}	2.830×10^{-7}	2.220×10^{-7}
0.8	1.620×10^{-7}	1.430×10^{-7}	1.130×10^{-7}	6.200×10^{-8}
0.9	1.300×10^{-8}	2.300×10^{-8}	3.900×10^{-8}	6.800×10^{-8}
1	3.590×10^{-7}	3.590×10^{-7}	3.590×10^{-7}	3.590×10^{-7}

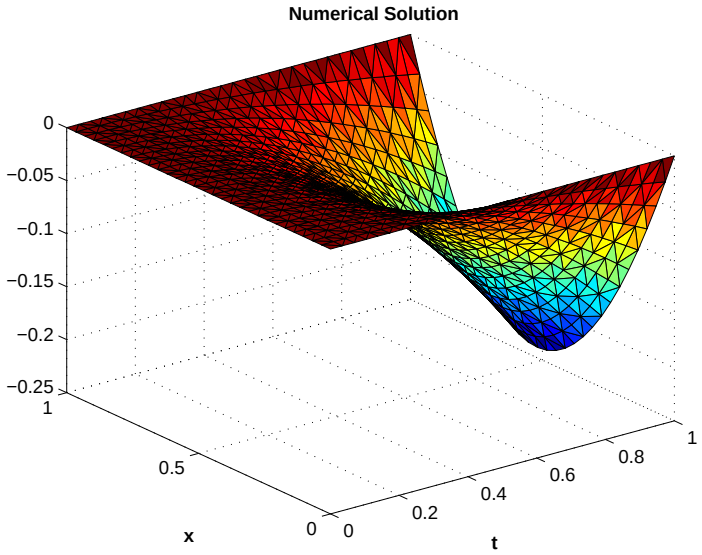

Figure 7. The numerical solution obtained using $N = 30$ nodes in global domain, $n = 5$ nodes in local domain, $M = 60$, and fractional order $\alpha = 1.85$.

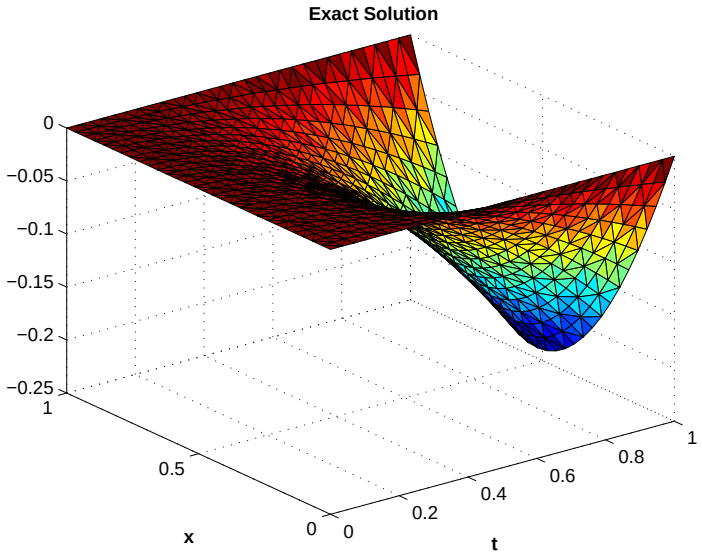

Figure 8. The exact solution obtained using $N = 30$ nodes in global domain, $n = 5$ nodes in local domain, $M = 60$, and fractional order $\alpha = 1.85$.

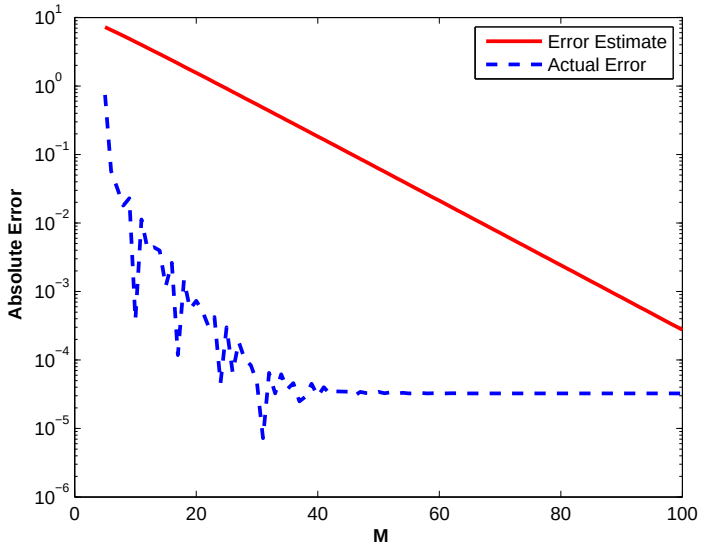

Figure 9. Plot of Actual error and Error Estimate corresponding to problem 2 obtained using $N = 80$ nodes in the global domain, $n = 10$ nodes in the local domain, fractional order $\alpha = 1.75$, at $t = 1$. The figure illustrate that the convergence rate of the numerical computation of inverse Laplace transform is inline with the Error Estimate (theoretical bound).

5.3. Problem 3

Here we consider the 1-D linear Klein-Gordon equation of the form [19]

$$\frac{\partial^\alpha \chi(x,t)}{\partial t^\alpha} = \frac{\partial^2 \chi(x,t)}{\partial x^2} + \chi(x,t),\ 0 \le \alpha \le 1,\ t \ge 0,\ x \in R, \tag{5.3}$$

with initial condition $\chi(x,0) = 1 + \sin(x)$ and exact solution $\chi(x,t) = \sin(x) + E_\alpha(t^\alpha)$, where $E_\alpha(t) = \sum_{m=0}^{\infty} \frac{t^m}{\Gamma(\alpha m+1)}$. The domain $[-4,4]$ is selected for the given problem. The quadrature points are generated using the MATLAB's command $\omega = -M : k : M$ along the path of integration Γ. The parameters used in our computations are $\alpha = 0.8, r = 0.1387, \eta = 2, \tau = \frac{t0}{T}, \theta = 0.1, \delta = 0.1541, t_0 = 0.5$ and $T = 5$. Using Eq (3.1) the remaining optimal parameters can be found for the hyperbolic path Γ. In our computations we select $n = 6$ centers in the sub domain Ω_i and $N = 40$ in the global domain Ω are selected. The error estimates and L_∞ errors are shown in Tables 6 and 7 . Similar behavior is observed as in the previous examples. The numerical and exact solutions for problem 3 are shown in Figures 10 and 11 and plot of Actual error and Error Estimate corresponding to problem 3 are shown in Figure 12.

Table 6. Approximate solution for Problem 3 at $t = 1$, and $1\times 10^{12} \leq \kappa \leq 1\times 10^{16}$, in the domain $[-4, 4]$.

$N = 70$, $n = 10$, $\alpha = 0.25$	M	L_∞ Error (Γ)	Error Estimate (Γ)	CPU time(s)
	10	7.37×10^{0}	4.4187	0.168655
	20	4.14×10^{-1}	1.5582	0.216721
	30	3.13×10^{-1}	0.5373	0.268500
	40	9.80×10^{-3}	0.1836	0.352215
	50	1.49×10^{-2}	0.0625	0.480307
	60	2.60×10^{-3}	0.0212	0.899249
	70	8.67×10^{-4}	0.0072	2.037757
	80	8.90×10^{-4}	0.0024	3.956089
	90	8.12×10^{-4}	8.18×10^{-4}	6.517429

Table 7. Approximate solution for Problem 3 at $t = 1$, and $1\times10^{12} \leq \kappa \leq 1\times 10^{16}$, in the domain $[-4, 4]$.

$N = 40$, $n = 6$, $\alpha = 0.8$	M	L_∞ Error (Γ)	Error Estimate (Γ)	CPU time(s)
	10	2.68×10^{0}	4.4187	0.158384
	15	4.53×10^{-1}	2.6363	0.162534
	20	3.36×10^{-1}	1.5582	0.162535
	30	1.59×10^{-1}	0.5373	0.189903
	40	2.0×10^{-3}	0.1836	0.245566
	50	8.70×10^{-3}	0.0625	0.344221
	60	1.10×10^{-3}	0.0212	0.502084
	70	6.32×10^{-4}	0.0072	0.923548
	80	5.70×10^{-4}	0.0024	2.520403

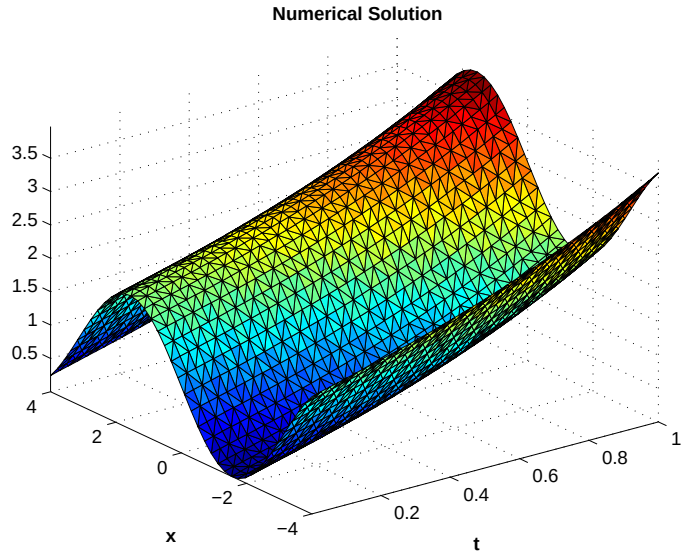

Figure 10. The numerical solution obtained using $N = 40$ nodes in global domain, $n = 8$ nodes in local domain, $M = 50$, and fractional order $\alpha = 0.9$.

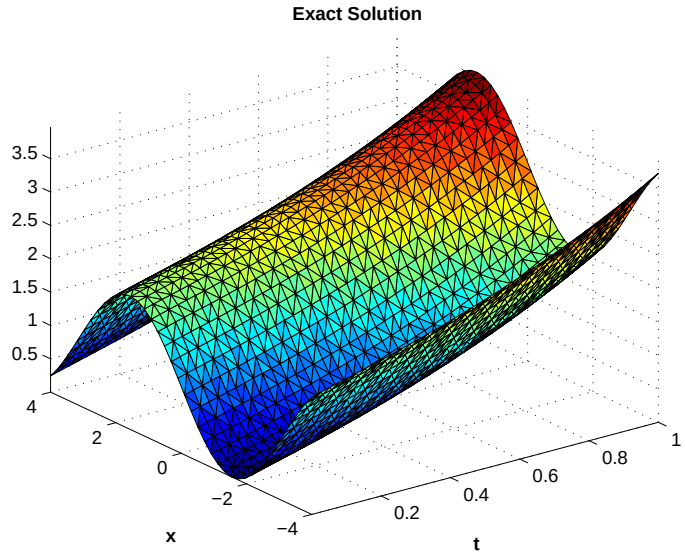

Figure 11. The exact solution obtained using $N = 40$ nodes in global domain, $n = 8$ nodes in local domain, $M = 50$, and fractional order $\alpha = 0.9$.

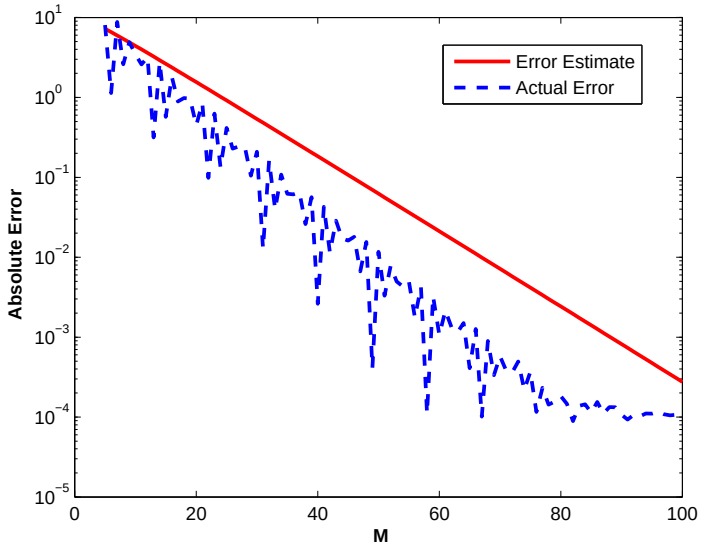

Figure 12. Plot of Actual error and Error Estimate corresponding to problem 3 obtained using $N = 70$ nodes in the global domain, $n = 10$ nodes in the local domain, fractional order $\alpha = 0.85$, at $t = 1$. The figure illustrate that the convergence rate of the numerical computation of inverse Laplace transform is inline with the Error Estimate (theoretical bound).

6. Conclusion

In this article, we constructed a local RBF method based on Laplace transform proposed for the approximation of the solution of the linear time fractional Klein-Gordon equations. In time stepping procedure usually the time instability is encountered and for accuracy we need a very small time step size. Global RBF methods are efficient and accurate only for small amount of nodes. They become inefficient and the differentiation matrix becomes ill-conditioned for large amount of nodes. The main advantage of this method is that it avoids the time stepping procedure with the help of Laplace transform, and the local RBF method has been used to resolve the issue of ill-conditioning. The numerical results confirmed the stability and convergence of the method. The comparison of the results with other methods led us to conclude that the proposed local RBF method coupled with Laplace transform is an efficient method for approximation of the solution of the linear time fractional Klein-Gordon equations.

Acknowledgments

The authors wish to thank the referees for their careful reading of the manuscript and valuable suggestions.This work was supported in part by the National Key Research and Development Program under Grant 2018YFB0904205, in part by the Key Laboratory of Pattern Recognition and Intelligent Information Processing , Institutions of Higher Education of Sichuan Province under Grant MSSB-2020-12.

Conflict of interest

The authors declare that no competing interests exist.

References

1. F. Yousef, M. Alquran, I. Jaradat, et al. *Ternary–fractional differential transform schema: Theory and application*, Adv. Differ. Equ., **2019** (2019), 1–13.
2. S. Bhatter, A. Mathur, D. Kumar, et al. *A new analysis of fractional Drinfeld–Sokolov–Wilson model with exponential memory*, Physica A, **537** (2020), 122578.
3. A. Goswami, J. Singh, D. Kumar, et al. *An efficient analytical approach for fractional equal width equations describing hydro–magnetic waves in cold plasma*, Physica A, **524** (2019), 563–575.
4. D. Kumar, F. Tchier, J. Singh, et al. *An efficient computational technique for fractal vehicular traffic flow*, Entropy, **20** (2018), 1–9.
5. D. Kumar, J. Singh, D. Baleanu, *On the analysis of vibration equation involving a fractional derivative with Mittag–Leffler law*, Math. Meth. Appl. Sci., **43** (2020), 443–457.
6. A. Yusuf, M. Inc, A. I. Aliyu, et al. *Efficiency of the new fractional derivative with nonsingular Mittag–Leffler kernel to some nonlinear partial differential equations*, Chaos Soliton Fract., **116** (2018), 220–226.
7. D. Kumar, J. Singh, K. Tanwar, et al. *A new fractional exothermic reactions model having constant heat source in porous media with power, exponential and Mittag-Leffler laws*, Int. J. Heat Mass Tran., **138** (2019), 1222–1227.
8. D. Kumar, J. Singh, S. D. Purohit, et al. *A hybrid analytical algorithm for nonlinear fractional wave–like equations*, Math. Model. Nat. Pheno., **14** (2019), 1–13.
9. M. J. Ablowitz, M. A. Ablowitz, P. A. Clarkson, et al. *Solitons, Nonlinear Evolution Equations and Inverse Scatterin*, Cambridge university press, 1991.
10. A. M. Yang, Y. Z. Zhang, C. Cattani, et al. *Application of local fractional series expansion method to solve Klein–Gordon equations on Cantor sets*, Abstr. Appl. Anal., **2014** (2014) , 1–6.
11. A. M. Wazwaz, *New travelling wave solutions to the Boussinesq and the Klein–Gordon equations*, Commun. Nonlinear Sci., **13** (2008), 889–901.
12. A. M. Wazwaz, *The tanh and the sine–cosine methods for compact and noncompact solutions of the nonlinear Klein–Gordon equation*, Appl. Math. Comput., **167** (2005), 1179–1195.
13. A. S. V. R. Kanth, K. Aruna, *Differential transform method for solving the linear and nonlinear Klein–Gordon equation*, Comput. Phys. Commun., **180** (2018), 708–711.
14. K. Hosseini, P. Mayeli, R. Ansar, *Modified Kudryashov method for solving the conformable time-fractional Klein–Gordon equations with quadratic and cubic nonlinearities*, Optik, **130** (2017), 737–742.
15. K. Hosseini, P. Mayeli, D. Kuma, *New exact solutions of the coupled sine-Gordon equations in nonlinear optics using the modified Kudryashov method*, J. Mod. Optic., **65** (2018), 361–364.

16. K. Hosseini, P. Mayeli, R. Ansar, *Bright and singular soliton solutions of the conformable time-fractional Klein–Gordon equations with different nonlinearities*, Wave. Random Complex, **28** (2018), 426–434.

17. K. Hosseini, Y. J. Xu, P. Mayeli, et al. *A study on the conformable time-fractional Klein–Gordon equations with quadratic and cubic nonlinearitiesA study on the conformable time-fractional Klein–Gordon equations with quadratic and cubic nonlinearities*, Optoelectron. Adv. Mat., **11** (2017), 423–429.

18. E. Yusufoğlu, *The variational iteration method for studying the Klein–Gordon equation*, Appl. Math. Lett., **21** (2008), 669–674.

19. M. Alaroud, M. Al-Smadi, O. A. Arqub, et al. *Numerical Solutions of Linear Time–fractional Klein–Gordon Equation by Using Power Series Approach*, SSRN Electron. J., **2018** (2018), 1–6.

20. M. Kurulay, *Solving the fractional nonlinear Klein–Gordon equation by means of the homotopy analysis method*, Adv. Differ, Equ., **2012** (2012), 1–8.

21. K. A. Gepreel, M. S. Mohamed, *Analytical approximate solution for nonlinear space–time fractional Klein–Gordon equation*, Chinese Phys. B, **22** (2013), 010201.

22. A. K. Golmankhaneh, A. K. Golmankhaneh, D. Baleanu, *On nonlinear fractional Klein–Gordon equation*, Signal Process., **91** (2011), 446–451.

23. E. A. B. Abdel-Salam, E. A. Yousif, *Solution of nonlinear space–time fractional differential equations using the fractional Riccati expansion method*, Math. Probl. Eng., **2013** (2013), 1–6.

24. D. Kumar, J. Singh, D. Baleanu, *A hybrid computational approach for Klein–Gordon equations on Cantor sets*, Nonlinear Dynam., **87** (2017), 511–517.

25. A. Mohebbi, M. Abbaszadeh, M. Dehghan, *High-order difference scheme for the solution of linear time fractional Klein–Gordon equations*, Numer. Meth. Part. Differ. Equ., **30** (2014), 1234–1253.

26. M. Dehghan, M. Abbaszadeh, A. Mohebbi, *An implicit RBF meshless approach for solving the time fractional nonlinear sine-Gordon and Klein–Gordon equations*, Eng. Anal. Bound. Elem., **50** (2015), 412–434.

27. M. M. Khader, *An efficient approximate method for solving linear fractional Klein–Gordon equation based on the generalized Laguerre polynomials*, Int. J. Comput. Math., **90** (2013), 1853–1864.

28. G. Hariharan, *Wavelet method for a class of fractional Klein-Gordon equations*, J. Comput. Nonlinear Dynam., **8** (2013), 1–6.

29. H. Singh, D. Kumar, J. Singh, et al. *A reliable numerical algorithm for the fractional klein-gordon equation*, Eng. Trans., **67** (2019), 21–34.

30. S. Vong, Z. Wang, *A compact difference scheme for a two dimensional fractional Klein–Gordon equation with Neumann boundary conditions*, Entropy, **274** (2014), 268–282.

31. M. Dehghan, A. Shokri, *Numerical solution of the nonlinear Klein–Gordon equation using radial basis functions*, J. Comput. Appl. Math., **230** (2009), 400–410.

32. M. Dehghan, A. Shokri, *A method of solution for certain problems of transient heat conduction*, AIAA J., **8** (1968), 2004–2009.

33. G. J. Moridis, D. L. Reddell, *The Laplace transform finite difference method for simulation of flow through porous media*, Water Resour. Res., **27** (1991), 1873–1884.
34. G. J. Moridis, D. L. Reddell, *The Laplace transform boundary element (LTBE) method for the solution of diffusion-type equations*, In: *Boundary Elements XIII*, Springer, Dordrecht, 1991, 83–97.
35. G. J. Moridis, D. L. Reddell, *The Laplace transform finite element (LTFE) numerical method for the solution of the ground water equations, paper H22C-4, AGU 91 Spring Meeting, Baltimore, May 28-31, 1991*, EOS Trans. of the AGU, **72** (1991), 17.
36. E. A. Sudicky, R. G. McLaren, *The Laplace Transform Galerkin Technique for large-scale simulation of mass transport in discretely fractured porous formations*, Water Resour. Res., **28** (1992), 499–514.
37. G. J. Moridis, E. J. Kansa, *The Laplace transform multiquadric method: A highly accurate scheme for the numerical solution of partial differentia*, J. Appl. Sci. Comput., (1993), 55910181.
38. Q. T. L. Gia, W. Mclean, *Solving the heat equation on the unit sphere via Laplace transforms and radial basis functions*, Adv. Comput. Math., **40** (2014), 353–375.
39. W. McLean, V. Thomee, *Time discretization of an evolution equation via Laplace transforms*, IMA J. Numer. Anal., **24** (2004), 439–463.
40. M. L. Fernandez, C. Palencia, *On the numerical inversion of the Laplace transform of certain holomorphic mappings*, Appl. Numer. Math., **51** (2004), 289–303.
41. W. McLean, V. Thomee, *Numerical solution via Laplace transforms of a fractional order evolution equation*, J. Integral Equ. Appl., **22** (2010), 57–94.
42. J. A. C. Weideman, L. N. Trefethen, *Parabolic and Hyperbolic contours for computing the Bromwich integral*, Math. Comput., **76** (2007), 1341–1356.
43. D. Sheen, I. H. Shaon, V. Thomee, *A parallel method for time discretization of parabolic equations based on Laplace transformation and quadrature*, IMA J. Numer.l Anal., **23** (2003), 269–299.
44. Z. J. Fu, W. Chen, H. T. Yang, *Boundary particle method for Laplace transformed time fractional diffusion equations*, J. Comput. Phys., **235** (2013), 52–66.
45. M. Uddin, A. Ali, *On the approximation of time-fractional telegraph equations using localized kernel–based method*, Adv. Differ. Equ., **2018** (2018), 1–14.
46. M. Uddin, A. Ali, *A localized transform–based meshless method for solving time fractional wave–diffusion equation*, Eng. Anal. Bound. Elem., **92** (2018), 108–113.
47. K. B. Oldham, J. Spanier, *The fractional calculus theory and applications of differentiation and integration to arbitrary order*, Academic Press, New York, London, 1974.
48. M. Uddin, *On the selection of a good value of shape parameter in solving time dependent partial differential equations using RBF approximation method*, Appl. Math. Model., **38** (2014), 135–144.
49. R. E. Carlson, T. A. Foley, *The parameter r^2 in multiquadric interpolation*, Comput. Math. Appl., **21** ((1991), 29–42.
50. R. E. Carlson, T. A. Foley, *Near optimal parameter selection for multiquadric interpolation*, Manuscript, Computer Science and Engineering Department, Arizona State University, Tempe., **20** (1994).

51. D. Kumar, F. Tchier, J. Singh, et al. *Error estimates and condition numbers for radial basis function interpolation*, Adv. Comput. Math., **3** (1995), 251–264.

52. L. N. Trefethen, D. Bau, *Numerical Linear Algebra*, SIAM, 1997.